Date: _October 26, 1977_

Project Title: _Determination of Ion-Neutral Interaction Potentials from Ion Drift Tube Data_

Project No: _G-41-663_

Project Director: _Dr. Ian R. Gatland_

Sponsor: _National Science Foundation; Washington, D.C. 20550_

Agreement Period: From _9/1/77_ Until _2/28/79*_
*12 months proposed period plus 6 months for flexibility

Type Agreement: _Grant No. CHE76-84181_

Amount:
$20,000 NSF Funds (G-41-663)
5,308 GIT Contribution (G-41-350)
$25,308 Total

Reports Required: _Annual Technical Letters; Summary of Completed Project; Final Technical Report_

Sponsor Contact Person (s):

Technical Matters	Contractual Matters
Maurice E. Schwartz	(thru OCA)
Associate Program Director	_Ms. Mary Frances O'Connell_
Quantum Chemistry Program	_Grants Administrator - Area 4_
Physical Chemistry & Dynamics Section	_National Science Foundation_
Division of Chemistry	_Washington, D. C. 20550_
National Science Foundation	_(202) 632-2858_
Washington, D. C. 20550	

Defense Priority Rating: _none_

Assigned to: _Physics_ (School/Laboratory)

COPIES TO:

Project Director	Library, Technical Reports Section
Division Chief (EES)	Office of Computing Services
School/Laboratory Director	Director, Physical Plant
Dean/Director—EES	EES Information Office
Accounting Office	Project File (OCA)
Procurement Office	Project Code (GTRI)
Security Coordinator (OCA)	Other_____
Reports Coordinator (OCA)	

CA—3 (3/76)

GEORGIA INSTITUTE OF TECHNOLOGY
OFFICE OF CONTRACT ADMINISTRATION

SPONSOR ROJECT TERMINATION

Date: 8/29/80

Project Title: Determination of Ion-Neutral Interaction Potentials from Ion Drift Tube Data

Project No: G-41-663

Project Director: I.R. Gatland

Sponsor: National Science Foundation

Effective Termination Date: 2/29/80 (Grant Period)

Clearance of Accounting Charges: 2/29/80

Grant/Contract Closeout Actions Remaining:

- _ Final Invoice and Closing Documents
- X Final Fiscal Report
- _ Final Report of Inventions
- _ Govt. Property Inventory & Related Certificate
- _ Classified Material Certificate
- _ Other _____

Assigned to: Physics (School/~~Laboratory~~)

COPIES TO:

Project Director
Division Chief (EES)
School/Laboratory Director
Oean/Director—EES
Accounting Office
Procurement Office
Security Coordinator (OCA)
Reports Coordinator (OCA)

Library, Technical Reports Section
EES Information Office
Project File (OCA)
Project Code (GTRI)
Other C. E. Smith

CA—4 (1/79)

GEORGIA INSTITUTE OF TECHNOLOGY
ATLANTA. GEORGIA 30332

(404) 894-5201

SCHOOL OF PHYSICS

September 22, 1978

Dr. John P. Lowe
Quantum Chemistry Program
National Science Foundation
Washington, D. C.   20550

Dear Dr. Lowe:

This is the annual technical letter for N.S.F. Grant No. CHE 76-84181 with project title "Determination of Ion-Neutral Interaction Potentials from Ion Drift Tube Data".

The personnel working on this project are myself, Ian R. Gatland, as project director and two graduate students; Mr. J. M. Cathcart and Mr. D. R. Lamm. Some of the work has also been done in collaboration with Dr. E. A. Mason of Brown University and Dr. L. A. Viehland of Parks College, St. Louis University.

The progress over the previous year (Sept. 1, 1977 to July 31, 1978) is detailed below by topic.

(a) The derivation of interaction potentials for Cs^+ - Ar, Cs^+ - Kr, and Cs^+ - Xe has been completed. These potentials are obtained directly from experimental data using the kinetic theory techniques proposed by Viehland and Mason.

(b) Interaction potentials have been derived directly from experiment for Rb^+ - Ar, Rb^+ - Kr, and Rb^+ - Xe. These potentials have been compared with the electron gas - Drude model potentials of Gordon and Waldman. This, together with results for other ion - gas combinations should help to refine the model calculations which, in turn, would influence the application of the model to neutral - neutral interactions of interest in excimer laser studies.

(c) The Cs^+ - Ar potential has been used to obtain mobilities for neutral gas temperatures of $77^\circ K$, $300^\circ K$, and $1000^\circ K$ in order to test a refined expression for obtaining the effective temperature from experimental data (see Ellis et al., At. Data, Nuc. Data Tables 17, (1976) 177).

(d) Studies of the Li^+ - H_2 system have been initiated with the development of a suitable expression for the symmetric part of the potential at both intermediate and long range.

(e) An established theoretical potential exists for H^+ - He (see Kotos and Peek, Chem. Phys. 12 (1976) 381) so this should provide a sensitive test of the kinetic theory. At low energies the comparison is very good but at high energies the interaction becomes Coulombic and the mobility does not exist. Further studies to elucidate this situation are under way.

(f) The kinetic theory in its present form cannot properly handle diffusion calculations since the difference between longitudinal and transverse diffusion implies that at least two temperatures must be associated with the ion motion. Including the neutral gas temperature this requires a "three temperature" theory. One such theory has been developed by Mason and Viehland and we are now testing it.

Both of the last two topics (e and f) are being carried out in conjunction with Drs. Mason and Viehland.

Many of the topics above are presently in progress and some others are due for study shortly. Topics for the next year include (d), (e), and (f) together with the following:

(g) Direct determination of interaction potentials for K^+ - Xe, K^+ - Kr, and possibly K^+ - Ne.

(h) Interaction potentials for Na^+ - Xe, Na^+ - Kr, Na^+ - Ar, Na^+ - Ne, and possibly Na^+ - He.

Besides the NSF grant I am also receiving partial support from ONR Grant No. N00014-76-0015. The work under the ONR grant is complementary to that listed above and consists of obtaining directly determined interaction potentials for various negative halogen ion-rare gas combinations. At present Cl^- - Xe has been completed and Cl^- - Kr is underway. Others with data ready for study include Br^- - Xe and F^- - Kr. The mobility data for F^- - Xe do not extend to high enough energies (E/N) to permit a potential to be obtained without incorporating other data or assuming a simple extrapolation. Experimental data for Br^- - Kr should be available in the near future.

The potentials obtained for F^- - Kr and Cl^- - Kr will also be compared with the electron gas - Drude model calculations of Kim and Gordon (Y. S. Kim and R. G. Gordon, J. Chem. Phys. 61, (1974) 1) to see where refinements are needed in their theory.

The potentials for Cs^+ - Ar, Cs^+ - Kr and Cs^+ - Xe, together with the mobilities, have been published (I. R. Gatland, M. G. Thackston, W. M. Pope, F. L. Eisele, H. W. Ellis, and E. W. McDaniel, J. Chem. Phys. 68, (1978) 2775) and a similar paper on Rb^+ - Ar, Rb^+ - Kr, and Rb^+ - Xe has been accepted for publication (I. R. Gatland, D. R. Lamm, M. G. Thackston, W. M. Pope, F. L. Eisele, H. W. Ellis, and E. W. McDaniel, J. Chem. Phys. 69, (1978) No. 11). Copies of these papers are enclosed.

Part of this work has been done in close collaboration with the drift tube experimental group, headed by Dr. McDaniel, which is responsible for much of the mobility data.

page 3
Dr. John P. Lowe
Washington, D. C. 20550
Sept. 22, 1978

   In conclusion I would like to thank the National Science Foundation for their support, and consequent encouragement, of this work.

<div style="text-align:right">

Yours sincerely,

Ian R. Gatland

</div>

IRG:ar

Enclosure

FINAL TECHNICAL REPORT

N S F   GRANT   CHE 76-84181

TITLE: "Determination of Ion-Neutral Interaction Potentials from Ion Drift Tube Data".

GRANT NO: CHE 76-84181, NSF

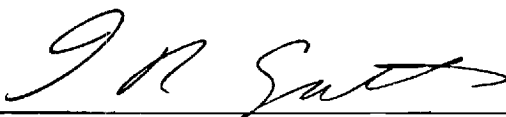PROJECT NO. G-41-663, Georgia Institute of Technology

PERIOD: 9/1/77 - 2/29/80

PERSONNEL: Ian R. Gatland, Project Director
Professor, School of Physics

D. R. Lamm, Graduate Student
J. M. Cathcart, Graduate Student

SUBMITTED: 2/29/80

I. R. Gatland

Please read instructions on reverse carefully before completing this form.

1. INSTITUTION AND ADDRESS		2. NSF PROGRAM	3. GRANT PERIOD
Georgia Institute of Technology Atlanta, Georgia 30332		Quantum Chemistry	9/1/77 - 2/29/80 *from*　　　*to*

4. GRANT NUMBER	5. BUDGET DUR. (MOS)	6. PRINCIPAL INVESTIGATOR(S)	7. GRANTEE ACCOUNT NUMBER
CHE76-84181	30	Ian R. Gatland	G-41-663

8. SUMMARY (Attach list of publications to form)

Ion drift tube experiments, in which ions gain momentum from an external electric field (E) and lose it via collisions with a neutral gas (density N), yield information about the ion-neutral interaction potential which controls the collisions. Using the theory of Viehland and Mason the average ion velocity, as a function of E/N, may be calculated for a specified potential. Further an iterative procedure has been developed so that potentials may be determined directly from drift tube experimental data.

These methods have been applied to test theoretical potentials and determine potentials which best fit the data for cesium and rubidium ions in argon, krypton, and xenon. The potentials so determined, being a fundamental description of the interaction, are of interest in studies of ion clustering in the upper atmosphere and lasing action in excimer lasers.

An unexpected result appeared in the case of protons in helium where, above a certain E/N, the calculations failed. Further study revealed that for this potential the collisions cannot remove momentum fast enough so the ions are forever accelerated and experience "run away" . This may have implications in tokamak design.

9. SIGNATURE OF PRINCIPAL INVESTIGATOR/ PROJECT DIRECTOR	TYPED OR PRINTED NAME	DATE
	Ian R. Gatland	2/29/80

N S F GRANT CHE 84181

"DETERMINATION OF ION-NEUTRAL INTERACTION

POTENTIALS FROM ION DRIFT TUBE DATA"

I. R. Gatland, Principal Investigator

School of Physics, Georgia Institute of Technology

PAPERS PUBLISHED WITH SUPPORT FROM THIS GRANT:

1. I. R. Gatland, M. G. Thackston, W. M. Pope, F. L. Eisele, H. W. Ellis, and E. W. McDaniel, J. Chem. Phys. 68, 2775 (1978)

2. I. R. Gatland, D. R. Lamm, M. G. Thackston, W. M. Pope, F. L. Eisele, H. W. Ellis and E. W. McDaniel, J. Chem. Phys. 69, 4951 (1978)

3. S. L. Lin, I. R. Gatland, and E. A. Mason, J. Phys. B. 12, 4179 (1979)

Description of Research

This research is concerned with the determination of various atomic and molecular properties associated with the interaction of ions with neutral particles. The primary experimental data is that derived from drift tube experiments, principally mobilities and diffusion coefficients.[1] Such experiments involve ion-neutral collisions at very low energies, typically less than 1 eV, and thus are particularly sensitive to the potential well part of the interaction. The long range part of the interaction is dominated by the polarization force, which is usually well known from other experiments[2], and the short range part may be determined by beam scattering experiments[3]. However, the results of drift tube experiments do not yield scattering information immediately. The ion drift is a somewhat random motion so that a range of ion-neutral collision energies and angles is associated with a single measurement. If the velocity distributions of the ions and neutrals are known then trial potentials may be tested by the data. Further if the potential is known to be symmetric and the data effectively cover a wide range of collision energies then information about the potential may be derived from the data[4]. However, except at very low collision energies, the ions are not in thermal equilibrium with the neutrals and their velocity distribution is far from Maxwellian.

This last consideration was the major barrier to the use of mobility data in the study of ion-neutral interaction potentials and was not overcome until the classic work of Viehland and Mason [5,6] in 1974. Their approach was to derive a moment solution of the Boltzmann equation using Burnett functions as a basis set in velocity space with the added critical feature that all velocities were normalized in terms of an effective temperature appropriate to the ion-neutral collisions. All the studies described here are based on a computational scheme derived from the Viehland-Mason theory. The expansion of the collision integral (and the other terms in the Boltzmann equation) over the basis set yields an infinite set of coupled algebraic equations and the definition of the effective temperature appears as a non-linear subsidiary equation. Numerical results are obtained by truncation and iteration of these equations. Application of these methods to various alkali ion-inert gas interaction potentials, based on electron gas-Drude model calculations, established the appropriateness and usefulness of the theory and calculations.[7]

The next significant step was the development of an inversion procedure so that potentials could be determined directly from drift tube mobility data. The method was based on that of Smith for neutral-neutral interactions and involves an iterative technique in which the experimental data is folded with the theoretical mobilities derived from a trial potential to produce a refined poetntial[8]. Both the original program, using ab initio SCF potentials, and the direct determination procedures were applied successfully ot the Li^+-He interaction potential[9].

During the period of this grant several other ion atom combinations have been investigated. The first set was Cs^+-Ar, Cs^+-Kr, and Cs^+-Xe.[10] Since no theoretical potentials were available only the directly determined potentials were of interest. These were developed from a range of trial potentials with different well depths and shapes. Amongst other results of this study it was gratifying to find that the best potential was selected unambiguously, the only uncertainties being those associated with the corresponding experimental errors. The well depths and positions given by the directly determined potentials also follow the general trend for alkali ion-inert gas combinations.

The other major set studied was Rb^+-Ar, Rb^+-Kr, and Rb^+-Xe. Initially mobilities were calculated using the electron gas-Drude model potentials of Gordan and Waldman and then these were used to start the inversion procedure. The directly determined potentials showed a shallower well at longer range than those of Gordon and Waldman in all three cases. The changes were typically about 10%.[11]

Several other areas of interest were looked at, including an ion-molecule case (Li^+-H_2) which is still under investigation. Also many improvements and refinements were added to the computational scheme so that it is now a standard operation and can be used by graduate students who are not yet familiar with the Boltzmann equation solution.

The most startling result of these studies, however, is the case of H^+-He. An accurate well established, potential for protons in helium has been given by Kolos and Peek and appears to be a good candidate to test the Viehland Mason theory.[12] For effective temperatures close to thermal, or somewhat above, the calculated mobilities agreed with the data to well within the experimental error but at higher effective temperatures nonsense results appeared. At first sight it appeared that the mobility increased as the driving force on the ions decreased. Subsequent calculations showed that the Viehland-Mason theory was not convergent and the higher order terms, which reflect the high energy tail of the velocity distribution, gave increasingly larger effects. More careful consideration of the form of the potential revealed the source of the trouble. For small internuclear separation distances the potential becomes almost Coulombic. Indeed this behavior is present at energies where inelastic effects are still negligible. However, such a potential does not support the concept of a mobility i.e. a balance of momentum gained from the external field and momentum lost by collisions. Rather the cross section falls faster thant the encounter rate increases and the ions are continously accelerated. Unfortunately, this effect is not obvious in a drift tube experiment since almost all such ions are undetected in a typical experimental configuration. An experiment was later carried out by Albritton, et al. with a modified apparatus and the existance of runaway ions was substantiated.[13] In particular, the diffusion coefficients show the same behavior as the mobility. Although the Viehland-Mason theory cannot predict where this behavior will become obvious it can give relations for systems with various masses. Thus using the H^+-He results one may predict the behavior for D^+-He. Experiments for deutenium in helium were in full agreement with these predictions.[14]

REFERENCES

1. G. M. Thomson, J. H. Schummers, D. R. James, E. Graham, I. R. Gatland, M. R. Flannery, and E. W. McDaniel, J. Chem. Phys. 58, 2404 (1973)

2. R. R. Teachout and R. T. Pack, Atomic Data 3, 195 (1971)

3. H. Inouye and S. Kita, J. Chem. Phys. 57, 1301 (1972)

4. E. W. McDaniel and E. A. Mason, "The Mobility and Diffusion of Ions in Gases", (Wiley, New York, 1973)

5. L. A. Viehland and E. A. Mason, Ann. Phys. (NY) 91, 499 (1975)

6. L. A. Viehland and E. A. Mason, Ann. Phys. (NY) 110, 287 (1978)

7. I. R. Gatland, L. A. Viehland and E. A. Mason, J. Chem. Phys. 66, 537 (1977)

8. E. B. Smith, Physica (Utr.) 73, 211 (1974)

9. I. R. Gatland, W. F. Morrison, H. W. Ellis, M. G. Thackston, E. W. McDaniel, M. H. Alexander, L. A. Viehland and E. A. Mason, J. Chem. Phys. 66, 5121 (1977)

10. I. R. Gatland, M. G. Thackston, W. M. Pope, F. L. Eisele, H. W. Ellis, and E. W. McDaniel, J. Chem. Phys. 68, 2775 (1978)

11. I. R. Gatland, D. R. Lamm, M. G. Thackston, W. M. Pope, F. L. Eisele, H. W. Ellis and E. W. McDaniel, J. Chem. Phys. 69, 4951 (1978)

12. W. Kołos and J. M. Peek, Chem. Phys. 12, 381 (1976)

13. F. Howorka, F. C. Fehsenfeld and D. L. Albritton, J. Phys. B. 12, 4189 (1979)

14. S. L. Lin, I. R. Gatland, and E. A. Mason, J. Phys. B. 12, 4179 (1979)

Mobility and diffusion of protons and deuterons in helium—a runaway effect

S L Lin†, I R Gatland‡ and E A Mason†

† Brown University, Providence, Rhode Island 02912, USA
‡ School of Physics, Georgia Institute of Technology, Atlanta, Georgia 30332, USA

Abstract. The mobility and diffusion of H^+ and D^+ ions in He gas are calculated classically, based on an accurate *ab initio* interaction potential. Comparison with corresponding quantal calculations of the zero-field mobility of H^+ in He as a function of temperature shows that quantum effects are negligible above 50 K, and are only 3% at 10 K. Calculations as a function of electric field strength at fixed gas temperature indicate a runaway effect, in which the ions cannot lose enough momentum by collisions to achieve a steady-state average velocity. The drift-tube measurements of Howorka *et al* are consistent with this interpretation. This appears to be the first report of runaway ions, although runaway electrons in plasmas are well known.

1. Introduction

The purpose of this paper is to present classical calculations of the mobility and diffusion of H^+ and D^+ ions in He gas. The ion–atom interaction potential has been calculated to such high accuracy by variational methods (Green *et al* 1974, Kołos 1976, Kołos and Peek 1976) that mobilities and diffusion coefficients are now calculable in principle to greater accuracy than they can be measured experimentally. Not only can the calculations as a function of temperature at vanishing electric field strength be performed very accurately (McDaniel and Mason 1973), but recent advances in kinetic theory now permit comparable accuracy in calculations as a function of field strength at fixed temperature (Viehland and Mason 1975, 1978).

After the present calculations were started, Dickinson and Lee (1978) reported quantum mechanical calculations of the mobility of H^+ in He as a function of temperature at vanishing field strength, using the accurate Kołos–Peek potential. Comparison of the present results with these allows a quantitative estimate of quantum effects on the mobility. Previous quantum mechanical calculations were based on a potential of substantially lower accuracy (Dickinson 1968), and previous classical calculations were based on even less accurate $(n, 4)$ potential models (Whealton *et al* 1974).

Our calculations were plagued by apparently poor convergence for values of E/N greater than about 25 Td (1 Td $\equiv 10^{-17}$ V cm^2), where E is the electric field strength and N is the number density of He atoms. The trouble is not computational, as originally suspected, but is the reflection of a real physical effect, in which the ion–atom momentum-transfer cross section decreases with increasing relative speed so quickly

that the ions are unable to lose enough momentum by collisions to achieve a steady-state drift velocity. As a result, the ions are continuously accelerated by the electric field, and no mobility exists. The diffusion coefficients are similarly ill-behaved. Recent measurements by Howorka *et al* (1979), reported in the following paper, are consistent with such a runaway effect. A similar runaway effect for electrons is known in plasma physics (Shkarofsky *et al* 1966), but this appears to be the first time the phenomenon has been reported for ions.

A simple criterion for the onset of the runaway effect can be given on the basis of momentum-transfer arguments. This criterion predicts how the onset changes as the ion mass is changed from H^+ to D^+, a result which is also confirmed by experiment (Howorka *et al* 1979).

2. Theory

The mobility K and drift velocity v_d are related to the ion–atom potential by the expression (Viehland and Mason 1975, 1978)

$$K \equiv \frac{v_d}{E} = \frac{3}{8} \frac{q}{N} \left(\frac{\pi}{2\mu k_B T_{eff}} \right)^{1/2} \frac{1+\alpha}{\bar{\Omega}^{(1,1)}(T_{eff})} \tag{1}$$

$$\tfrac{3}{2} k_B T_{eff} = \tfrac{3}{2} k_B T + \tfrac{1}{2} M v_d^2 (1+\beta) \tag{2}$$

where q is the ion charge, μ is the reduced mass of the ion–atom pair, k_B is Boltzmann's constant, T is the gas temperature, T_{eff} is an effective temperature that characterises the mean ion energy in the centre-of-mass frame of the ion–atom pairs, M is the atom mass (m is the ion mass), and α and β are corrections, zero in first approximation, that include all the higher kinetic-theory approximations. The momentum-transfer collision integral depends on T_{eff} and the ion–atom potential, and is defined as

$$\bar{\Omega}^{(1,1)}(T_{eff}) = \frac{1}{2(k_B T_{eff})^3} \int_0^\infty \exp(-\epsilon/k_B T_{eff}) \epsilon^2 Q^{(1)}(\epsilon) \, d\epsilon \tag{3}$$

where ϵ is the relative energy of an ion–atom collision and $Q^{(1)}$ is the momentum-transfer cross section,

$$Q^{(1)}(\epsilon) = 2\pi \int_0^\pi (1-\cos\theta)\sigma(\epsilon,\theta)\sin\theta \, d\theta \tag{4}$$

in which $\sigma(\epsilon,\theta)$ is the differential cross section for elastic scattering through an angle θ. The foregoing formulae hold whether $\sigma(\epsilon,\theta)$ and $Q^{(1)}(\epsilon)$ are calculated by classical or quantum mechanics. The normalisation factors in (3) and (4) are chosen so that both $Q^{(1)}$ and $\bar{\Omega}^{(1,1)}$ are equal to πd^2 for the classical collisions of rigid spheres of mutual diameter d.

The correction terms α and β depend on the ion and atom masses, the ion–atom potential, and T_{eff}. At vanishing electric fields β can be ignored and α usually amounts at most to a few per cent. At high fields both α and β are more important, but in most cases are still fairly small compared with unity. The present systems are an exception to this rule, since the runaway effect appears, in this theory, as large values of α and β that vary erratically in successive orders of approximation, indicating the inability of the kinetic theory to describe the physics of the situation.

Approximate scaling rules that account for the change of the K versus E/N curve when the ion mass is changed can readily be obtained from (1) and (2). Ignoring the term α, we see from (1) that $\mu^{1/2}K$ versus T_{eff} should give a single curve for both H^+ and D^+, assuming the ion–atom potential is independent of nuclear mass. If T is fixed and E/N is varied, then (2) shows that T_{eff} can be replaced by $(T_{\text{eff}} - T)$. However, T_{eff} is not the same for H^+ and D^+ at the same value of E/N, because of the second term in (2). Ignoring β, we see from (2) that $(T_{\text{eff}} - T)$ is proportional to $v_d^2 = K^2E^2$; since μK^2 depends only on T_{eff}, it follows that E^2/μ depends only on T_{eff} if T is fixed. We conclude that $\mu^{1/2}K$ versus $\mu^{-1/2}E/N$ is a single curve for both H^+ and D^+ at fixed T, and results for both systems can thus, conveniently, be presented together.

3. Numerical calculations

Given the ion–atom potential, the first steps are the calculation of $Q^{(1)}(\epsilon)$, $\bar{\Omega}^{(1,1)}(T_{\text{eff}})$, and a number of similar cross sections and collision integrals that are needed to calculate the correction terms α and β. The numerical integration procedures used have been described elsewhere (Gatland *et al* 1977), and the results were checked at various values of T_{eff} by means of an independent computer program (O'Hara and Smith 1971). The uncertainties in the collision integrals are estimated to be less than 0·2%, which is about the same accuracy achieved by Dickinson and Lee (1978) in their quantal calculations.

3.1. Zero-field mobility

For $E/N \to 0$, the mobility and diffusion coefficients are related by the Einstein relation, and can be calculated by standard Chapman–Enskog theory (McDaniel and Mason 1973). Convergence is very rapid, and the correction α never exceeds 0·2% below 800 K. It rises to about 3% at 5000 K as a result of the softness of the repulsive wall of the potential; this feature of the potential is also responsible for the runaway effect, as discussed later.

Results are shown in figure 1 for the mobility of H^+ in He at standard gas density. Agreement with the quantal calculations is well within the numerical uncertainties above about 50 K; below 50 K the quantum deviations become important, but still amount to only about 3% at 10 K. Agreement with the experimental value at 300 K is also within the experimental uncertainty of about 1% (Orient 1971, Howorka *et al* 1979). The mobility of D^+ in He at 300 K (Orient 1972, Howorka *et al* 1979), scaled according to $\mu^{1/2}$, also agrees within the 1% experimental uncertainty. Since quantum corrections are negligible above 50 K, any deviations from the $\mu^{1/2}$ scaling law at 300 K are due to the correction α, which is too small to have a noticeable effect.

The steady decrease of the classical mobility from its polarisation value at $T = 0$ K is caused by attractive interactions of shorter range than the r^{-4} polarisation potential. The charge-induced quadrupole energy, varying as r^{-6}, appears first, followed by the strong valence attraction that leads to a binding energy of 2·0 eV for HeH^+.

The temperature at which quantum deviations become appreciable for D^+ in He can be estimated from the results for H^+ in He by means of a mass-scaling rule, on the assumption that the interaction potentials are identical. The quantum deviations depend on the ratio λ/d, where $\lambda = h/(2\pi\mu kT)^{1/2}$ is the thermal de Broglie wavelength and d is some parameter that measures the range of the interaction. The initial
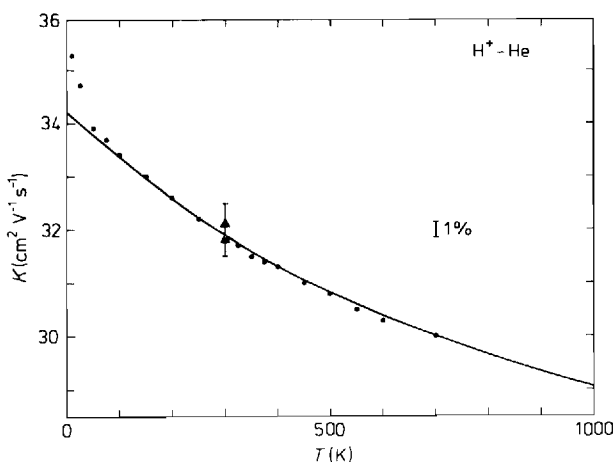
Figure 1. Zero-field mobility of H^+ in He as a function of temperature. Full curve, present classical calculations; full circles, quantum mechanical calculations (Dickinson and Lee 1978). Open triangle, measurement of Orient (1971); full triangle, scaled measurement for D^+ in He (Orient 1972).

quantum deviations for D^+–He will therefore be about the same as those for H^+–He at a temperature at which the two values of λ are the same. Thus the temperature at which quantum deviations first become appreciable will vary as $T \sim \mu^{-1}$.

3.2. Dependence on field strength

The calculations of mobility and diffusion coefficients as a function of field strength are more complicated because of slower convergence—that is, the corrections α and β are larger. We use a moment solution of the Boltzmann equation, with a truncation–iteration scheme for the infinite set of moment equations suggested by Viehland and Mason (1978), somewhat modified for faster convergence (Lin and Mason 1979).

The mobility results at 300 K as a function of E/N for both H^+ and D^+ in He are shown in figure 2, scaled on both axes according to the $\mu^{1/2}$ rules discussed in § 2. Since M is fixed, it is more convenient to use the dimensionless quantity $m/(m + M)$ in place of μ. The scaling is exact in the first approximation, where α and β are both zero, but deviations can be seen in the higher approximations. The experimental data follow the scaling well within the estimated experimental uncertainty of 5% (maximum), as well as agreeing in absolute value with the calculations at lower field strengths, below the onset of runaway. Comparison of the fourth and fifth approximations with the first approximation indicates that the mobilities converge to a definite limit below a scaled field strength of about $[(m + M)/m]^{1/2} (E/N) = 40$ Td. Between 40 and 55 Td, the small differences between the fourth and fifth approximations are probably due to slower convergence. Above about 60 Td, we attribute the differences to the runaway effect, and do not expect true convergence to occur even if higher approximations were to be calculated.

The experimental data (Howorka *et al* 1979) show runaway behaviour only above about 80 Td (scaled), rather higher than the 60 Td indicated by the calculations. This difference is not surprising, since the experiments and calculations are sensitive in
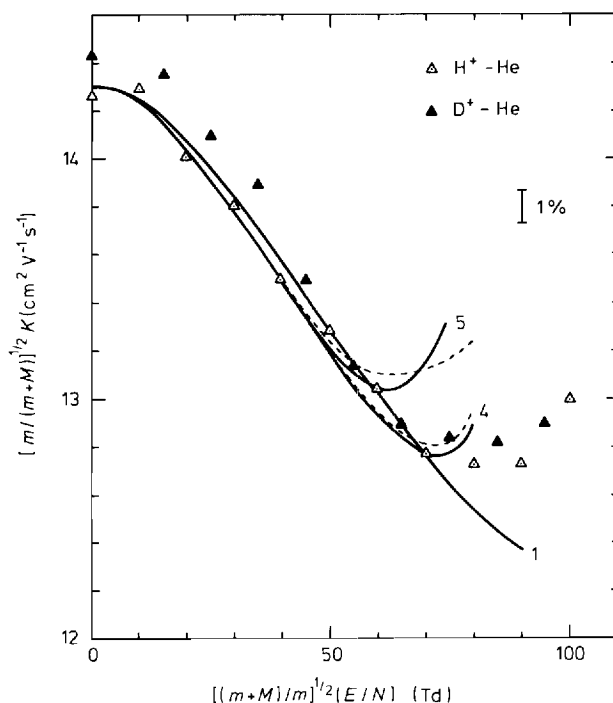
Figure 2. Mass-scaled mobilities of H^+ and D^+ in He at 300 K as a function of mass-scaled field strength, showing the onset of runaway. The curves are the present calculations, full curves for H^+ and broken curves for D^+. The numbers refer to the order of approximation. The triangles are smoothed values taken from the measurements of Howorka *et al* (1979).

different degrees to the high-velocity tail of the ion distribution function, where the runaway ions originate. A more quantitative discussion is given in the next section.

Our calculations also show unstable solutions for the diffusion coefficients, both parallel and perpendicular to the field direction. The experimental results at present are only qualitative, but do show a marked increase in the parallel diffusion coefficient for D^+ in He at about $E/N = 70$ Td (Howorka *et al* 1979). The onset of runaway is more difficult to see in the calculations for diffusion than for mobility, because the diffusion coefficients normally increase quite rapidly with E/N, in a roughly quadratic fashion (McDaniel and Mason 1973, pp 126–97). To remove this quadratic background and to normalise the diffusion coefficient to unity at $E/N = 0$, we can define reduced diffusion coefficients $\tilde{D}_{\parallel}$ and $\tilde{D}_{\perp}$ as

$$\tilde{D}_{\parallel,\perp} \equiv qD_{\parallel,\perp}/K(0)k_B T_{\text{eff}}(0) \tag{5}$$

where $K(0)$ is the zero-field mobility at fixed gas temperature T, and $T_{\text{eff}}(0)$ is given by

$$\tfrac{3}{2}k_B T_{\text{eff}}(0) \equiv \tfrac{3}{2}k_B T + \tfrac{1}{2}M(K(0)E)^2. \tag{6}$$

This expression for $T_{\text{eff}}(0)$ is analogous to that for T_{eff} given by (2), but uses $K(0)$ in place of K in $v_d = KE$ to avoid introducing peculiarities from the runaway behaviour of K itself. These reduced diffusion coefficients vary relatively slowly with increasing E/N, until unstable solutions occur.

Calculated values of $\tilde{D}_\parallel$ and $\tilde{D}_\perp$ at 300 K are shown in figure 3 as a function of mass-scaled field strength. Several effects can be noticed. Firstly, unstable solutions appear for $D_\parallel$ and $D_\perp$ at roughly the same field strengths as for mobility. Secondly, the convergence is somewhat poorer for diffusion than for mobility. This effect is a result of the particular moment solutions used, and is expected (Viehland and Mason 1978, Lin *et al* 1979). Thirdly, the simple scaling rule used on E/N is not as good for diffusion as for mobility, and the deviations are in opposite directions for $D_\parallel$ and $D_\perp$ (i.e. the results are higher for D^+ than for H^+ in one case and lower in the other). This result occurs because the diffusion coefficients do not depend just on the total random ion energy (i.e. on T_{eff}), but on the component of the random ion energy in their direction. The deviations in figure 3 are primarily mass effects, although the interaction plays some role. That is, the partitioning of the random ion energy between the directions parallel and perpendicular to the field depends primarily on the ion mass, according to both the simple formulae of Wannier (1953, see also McDaniel and Mason 1973), and to more elaborate formulae (Viehland *et al* 1974). These formulae show that the heavier ion has a greater fraction of its random energy parallel to the field than perpendicular to it, so that $\tilde{D}_\parallel$ is larger for D^+ than for H^+, and vice versa for $\tilde{D}_\perp$, as plotted in figure 3.
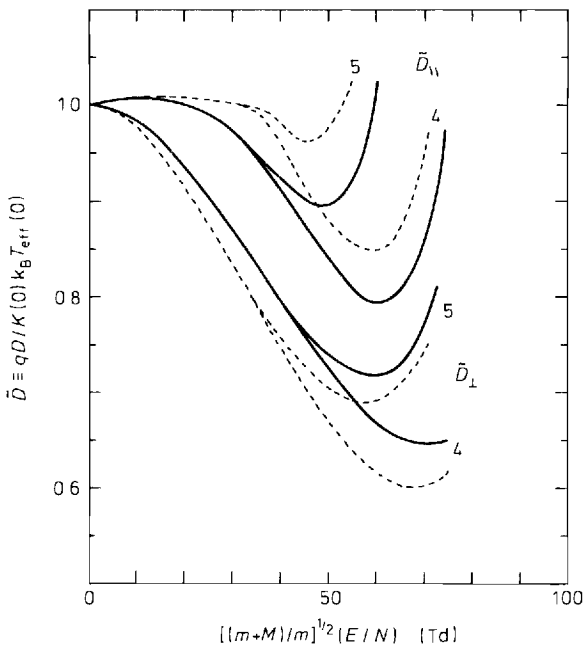

Figure 3. Scaled parallel and perpendicular diffusion coefficients for H^+ and D^+ in He, calculated at 300 K as a function of mass-scaled field strength, showing the onset of runaway. The full curves refer to H^+ and the broken curves to D^+. The numbers refer to the order of approximation.

4. Runaway ions

The runaway effect can be understood rather simply by momentum-transfer arguments (McDaniel and Mason 1973, § 5.2). The average momentum acquired by an ion from the field in unit time is qE, which must be balanced by an average momentum loss by

collisions with the neutral atoms, if a steady state is to occur. The average momentum loss to the gas per collision is proportional to $\mu v_d(1 - \cos \theta)$, and the average number of collisions an ion makes per unit time that scatter into an angle θ is $N\bar{v}2\pi\sigma(\bar{v}, \theta)\,d\theta$, where $\bar{v}$ is the mean relative ion–atom speed. Multiplying these two factors together and integrating over scattering angles, we find that the average collisional momentum loss per unit time by an ion is (within a factor of order unity)

$$\mu v_d N\bar{v}Q^{(1)}(\bar{v}) \tag{7}$$

where $Q^{(1)}(\bar{v})$ is the momentum-transfer cross section of (4), written in terms of $\bar{v}$ rather than ϵ. To relate v_d to $\bar{v}$, we note that the mean ion energy, $\frac{1}{2}m\overline{v^2}$, consists of a directed portion, $\frac{1}{2}mv_d^2$, plus a random portion given essentially by (2),

$$\tfrac{1}{2}m\overline{v^2} = \tfrac{1}{2}mv_d^2 + \tfrac{3}{2}k_B T + \tfrac{1}{2}Mv_d^2. \tag{8}$$

Neglecting the thermal energy and taking $\overline{v^2} \simeq \bar{v}^2$, we substitute for v_d in (7) and write for the momentum loss

$$2N[m/(m+M)]^{1/2}\epsilon Q^{(1)}(\epsilon) \tag{9}$$

where $\epsilon = \frac{1}{2}\mu\bar{v}^2$.

From (9) we can write an approximate criterion for the runaway as

$$[(m+M)/m]^{1/2}(E/N) > 2\epsilon Q^{(1)}(\epsilon). \tag{10}$$

When this condition holds, the ions cannot lose momentum by collisions as fast as they acquire it from the field. Usually $\epsilon Q^{(1)}$ continues to rise with increasing ϵ and does not have an absolute maximum within the range of normal drift-tube energies (although it may show a local one), so that this criterion cannot be met and runaway cannot occur. This is not the case for H^+–He or D^+–He, however, as shown in figure 4. The curve never rises higher than about 110×10^{-17} eV cm^2, so that virtually every ion will eventually run away when the mass-scaled field strength, $[(m+M)/m]^{1/2}(E/N)$, is greater than about 220 Td.

The curve of $\epsilon Q^{(1)}$ versus ϵ for H^+–He can be contrasted with that for an $(8, 4)$ potential having the same depth and position of the potential well, and nearly the same r^{-4} long-range polarisation tail. The $(8, 4)$ potential (Hassé and Cook 1929, see also McDaniel and Mason 1973) is shown in figure 4 as a broken curve, and after a first local maximum near $\epsilon = 1$ eV, the curve continues to rise, whereas the H^+–He curve shows a second maximum at about $\epsilon = 10^2$ eV and then falls off. This fall-off is caused by the softness of the repulsive wall of the potential. The shape of the $\epsilon Q^{(1)}(\epsilon)$ curve can be correlated with the potential as follows. At low energies the collisions are dominated by the r^{-4} polarisation potential, for which $Q^{(1)}(\epsilon)$ varies as $\epsilon^{-1/2}$. Thus $\epsilon Q^{(1)}(\epsilon)$ rises until a shorter-ranged repulsion manifests itself. There is initially a partial cancellation, leading to the first local maximum, and then the repulsion begins to dominate the scattering, leading to a minimum and subsequent rise in $\epsilon Q^{(1)}(\epsilon)$. Usually this rise continues to very high energies, but for H^+–He the short-range repulsion becomes so soft that $Q^{(1)}(\epsilon)$ falls more rapidly than ϵ^{-1} at high ϵ. The result is a second local maximum in $\epsilon Q^{(1)}(\epsilon)$ and a subsequent fall.

A criterion for the *absence* of runaway can therefore be stated as follows: at high energies $Q^{(1)}$ must decrease less rapidly than ϵ^{-1}. This is consistent with the results for electrons of Cavalleri and Paveri-Fontana (1972), whose discussion can also be applied to ions.
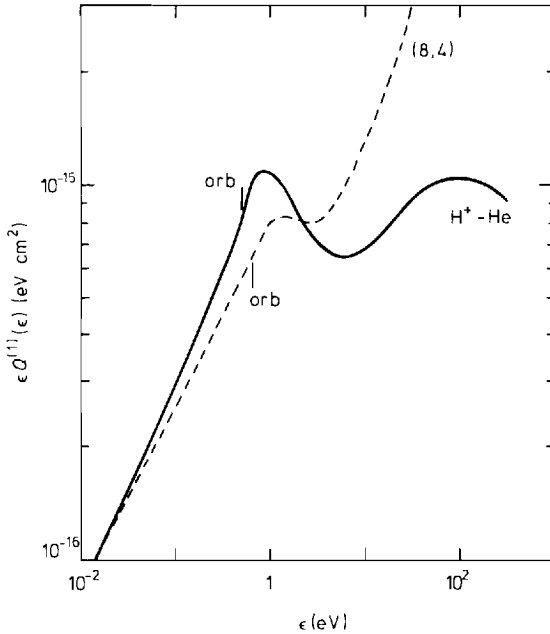
Figure 4. Collisional momentum loss as a function of relative collision energy, showing the conditions for runaway. Full curve, calculated for the actual H^+–He potential; broken curve, calculated for the $(8, 4)$ potential model. The energy limits for orbiting collisions are marked for both potentials.

The softness of the repulsive wall of the H^+–He interaction as compared to that of an $(8, 4)$ potential can also be seen by noting the value of separation for which the interaction is zero, taking the separation of maximum attraction to be $1 \cdot 463$ a_0 for both potentials. The zero occurs at $1 \cdot 230$ a_0 for the $(8, 4)$ potential, but at $1 \cdot 0$ a_0 for the H^+–He potential.

The criterion (10) for runaway has the same mass-scaling factor for E/N as given by (1) and (2) for no runaway. We thus expect the mass-scaling rules to hold even after the onset of runaway. The results shown in figure 2, both theoretical and experimental, are consistent with this expectation.

Some runaway ions will occur even for field strengths much less than that given by (10), since a few ions will have energies greater than that required for exact momentum balance. Such high-energy ions are usually kept small in number because the momentum loss by collisions increases with increasing energy, as illustrated by the $(8, 4)$ curve in figure 4. This is not the case for H^+–He; figure 4 shows that the collisional momentum loss is never more than its value at $\epsilon \simeq 0 \cdot 9$ eV. Thus there is no penalty of high momentum loss for an ion with high energy, and the ion distribution function develops a comparatively large high-energy tail. This furnishes a reservoir to replenish the ions of very high energy that pass over both local maxima shown in figure 4, and the high-energy ions are fated to be accelerated forever by the field. This long high-energy tail has been calculated explicitly by Rebentrost (1972) for the case of the cross section varying as ϵ^{-1}; the distribution decays as an inverse power of ϵ instead of exponentially. This means that the higher velocity moments of the distribution function will become infinite, and a moment solution for the distribution will encounter convergence difficulties.

The high-energy tail of the distribution function also accounts, at least qualitatively, for the different ways in which the onset of runaway is perceived. As higher approximations are taken in the moment solution, higher moments of the distribution are included in the set of equations to be solved. Since higher moments reach further into the tail of the distribution, convergence difficulties appear sooner as higher moments are included. Such behaviour can be seen in figure 4. However, drift-tube experiments are not likely to sense anything peculiar until a fairly large fraction of the ions are in the tail of the distribution, so that the onset of runaway seems to occur at higher E/N than is the case for the theoretical calculations.

5. Discussion

The present calculations, when compared with the quantal calculations of Dickinson and Lee (1978), show at what temperatures the quantum deviations become appreciable for the zero-field mobility of H^+ in He. Of more interest is the fact that the calculations indicate the onset of runaway behaviour when the gas temperature is held fixed and the electric field strength is increased. A simple momentum-balance equation explains the essential reason for the runaway ions in terms of the energy dependence of the momentum-transfer cross section. Mass-scaling rules for the isotope D^+ appear to work well.

Although the softness of the repulsive wall of the potential is responsible ultimately for the runaway behaviour, a partial cancellation of the effects of the attractive and repulsive components of the potential makes the runaway observable at a much lower energy. In terms of figure 4, the maximum in $\epsilon Q^{(1)}(\epsilon)$ at about 100 eV allows runaway to occur, but the cancellation effect is responsible for the first maximum at about 0·9 eV. The experimental observation of the rise of the mobility (Howorka *et al* 1979) is initiated by the fall of $\epsilon Q^{(1)}(\epsilon)$ above 0·9 eV, and is then accompanied by runaway behaviour according to the reasoning in § 4.

Runaway ions cannot be accelerated indefinitely in normal drift-tube experiments. If they do not come to the end or sides of the drift tube too soon, they will eventually begin to lose momentum through various inelastic channels that open up at high energies, such as electronic excitation and ionisation of the He atoms in the present case.

Acknowledgments

References

Cavalleri G and Paveri-Fontana S L 1972 *Phys. Rev.* A **6** 327–33
Dickinson A S 1968 *J. Phys. B: Atom. Molec. Phys.* **1** 395–401

Dickinson A S and Lee M S 1978 *J. Phys. B: Atom. Molec. Phys.* **11** L377–9
Gatland I R, Viehland L A and Mason E A 1977 *J. Chem. Phys.* **66** 537–41
Green T A, Michels H H, Browne J C and Madsen M M 1974 *J. Chem. Phys.* **61** 5186–97
Hassé H R and Cook W R 1929 *Proc. R. Soc.* A **125** 196–221
Howorka F, Fehsenfeld F C and Albritton D L 1979 *J. Phys. B: Atom. Molec. Phys.* **12** 4189–97
Kołos W 1976 *Int. J. Quantum Chem.* **10** 217–24
Kołos W and Peek J M 1976 *Chem. Phys.* **12** 381–6
Lin S L and Mason E A 1979 *J. Phys. B: Atom. Molec. Phys.* **12** 783–9
Lin S L, Viehland L A and Mason E A 1979 *Chem. Phys.* **37** 411–24
McDaniel E W and Mason E A 1973 *The Mobility and Diffusion of Ions in Gases* (New York: Wiley)
O'Hara H and Smith F J 1971 *Comput. Phys. Commun.* **2** 47–54
Orient O J 1971 *J. Phys. B: Atom. Molec. Phys.* **4** 1257–66
—— 1972 *J. Phys. B: Atom. Molec. Phys.* **5** 1056–8
Rebentrost F 1972 *Chem. Phys. Lett.* **17** 486–8
Shkarofsky I P, Johnston T W and Bachynski M P 1966 *The Particle Kinetics of Plasmas* (Reading, Mass.: Addison-Wesley) §§ 8–10
Viehland L A and Mason E A 1975 *Ann. Phys., NY* **91** 499–533
—— 1978 *Ann. Phys., NY* **110** 287–328
Viehland L A, Mason E A and Whealton J H 1974 *J. Phys. B: Atom. Molec. Phys.* **7** 2433–9
Wannier G H 1953 *Bell Syst. Tech. J.* **32** 170–254
Whealton J H, Mason E A and Vu T H 1974 *Chem. Phys. Lett.* **28** 125–9

Mobilities and interaction potentials for Rb$^+$–Ar, Rb$^+$–Kr, and Rb$^+$–Xe[a]

I. R. Gatland, D. R. Lamm, M. G. Thackston, W. M. Pope, F. L. Eisele, H. W. Ellis, and E. W. McDaniel

School of Physics, Georgia Institute of Technology, Atlanta, Georgia 30332
(Received 18 August 1978)

The mobilities of Rb$^+$ ions in Kr and Xe gases have been measured at 300°K in a drift tube mass spectrometer over a wide range of the ionic energy parameter E/N (the ratio of the electric field intensity to the neutral gas number density). The Viehland–Mason kinetic theory of ionic mobility (valid for arbitrary E/N) is used to derive theoretical mobilities from the electron gas-Drude model potentials of Gordon and Waldman for Rb$^+$–Ar (mobilities measured previously), Rb$^+$–Kr, and Rb$^+$–Xe. The results are compared with the experimental data. Further, by using an iterative technique, new potentials are developed which are determined directly by the experimental data, and these "experimental" potentials are tabulated and compared with the Gordon–Waldman potentials.

INTRODUCTION

We are concerned here with the mobility K of a species of ion drifting under steady-state conditions through a neutral gas in which a uniform, constant electric field of intensity E has been established. The mobility is defined by the equation $K = v_d/E$, where v_d is the drift velocity of the ions. Since the mobility is determined by ion–neutral scattering events, it is intimately related to the ion–neutral interaction potential.[1,2] Other factors affecting the mobility are the ion and neutral masses, the gas temperature, and the value of the ionic energy parameter E/N (here, N is the number density of the neutral gas). If these factors are known and if the ion–neutral potential is spherically symmetric, a knowledge of the potential is sufficient for calculation of K.[3,4] At present, it is not possible to utilize mobility data as a function of E/N to calculate analytically the ion–neutral potential as a function of the ion–neutral separation distance. However, an iterative inversion technique has been developed to obtain a potential which accurately reproduces the mobility data. We have studied the Li$^+$–He combination in this fashion,[3] and obtained a potential that compares favorably with various *ab initio* theoretical potentials computed for the Li$^+$–He system. Here, we report measurements of the mobilities of Rb$^+$ ions in Kr and Xe gases over a wide range of E/N at 300 °K, and, together with the previous results for Rb$^+$–Ar,[5] we use these data to derive interaction potentials for Rb$^+$–Ar, Rb$^+$–Kr, and Rb$^+$–Xe. The resulting potentials are compared with theoretical potentials.

EXPERIMENT

The drift tube mass spectrometer in which our measurements were made has been described in detail,[6,7] and our experimental techniques have also been discussed at length.[6,7] Hence, only a brief description will be presented here. Rb$^+$ ions, along with ions of other alkalis, are produced by thermionic emission from a coated filament inside an ion source that can be posi-

tioned at a number of different sites along the axis of the cylindrical drift tube. Short, periodic bursts of ions are gated from the source, and each burst drifts and diffuses a known distance along the axis through a neutral gas at constant temperature and pressure in a uniform, constant electric field. A small fraction of the ions in each burst then passes through an exit aperture at the end of the drift tube into a high vacuum region, where Rb$^+$ ions are mass selected by a quadrupole mass spectrometer and then detected by a single-particle counter.

We measure the time between the release of each Rb$^+$ ion from the ion source and its detection in the counter. The differences between the average flight times for various drift distances determine the drift velocity v_d and hence the mobility K. The mobility is inversely proportional to the number density of the neutral gas and, following convention, we normalize our results to the density at 760 torr and 0°C. The result is the "reduced mobility" K_0, where $K_0 = K(P/760)(273.16/T)$, and P and T are the pressure and temperature of the neutral gas in torr and °K, respectively. By using several ion source positions (thereby changing the drift distance) and taking differences in flight times, we eliminate a
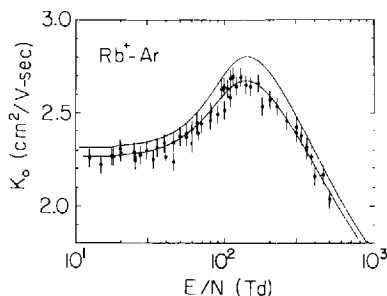

FIG. 1. The reduced mobility of Rb$^+$ ions in argon gas at 300 °K as a function of E/N in townsends (1 Td $= 10^{-17}$ V cm^2). The experimental data are shown as points. The upper curve is the result of calculations using the Gordon–Waldman theoretical potential. The lower curve is the result of calculations using the directly determined potential given in Table I. Extrapolation to zero electric field yields a reduced mobility of 2.26, compared to the polarization limit mobility of 2.077 (all mobilities in cm^2/V sec).

TABLE I. Interaction potential as a function of internuclear separation distance (both in a. u.: 27.21 eV and 0.529 Å) for Rb⁺–Ar, Rb⁺–Kr, and Rb⁺–Xe, obtained by direct inversion of mobility data.

Separation distance	Rb⁺–Ar	Rb⁺–Kr	Rb⁺–Xe
50.0	$-0.89530E-06$	$-0.13560E-05$	$-0.21938E-05$
35.0	$-0.37634E-05$	$-0.57067E-05$	$-0.92483E-05$
25.0	$-0.14710E-04$	$-0.22352E-04$	$-0.36339E-04$
20.0	$-0.36618E-04$	$-0.55770E-04$	$-0.90986E-04$
15.0	$-0.12055E-03$	$-0.18446E-03$	$-0.30305E-03$
14.0	$-0.16101E-03$	$-0.24673E-03$	$-0.40627E-03$
13.0	$-0.22013E-03$	$-0.33794E-03$	$-0.55794E-03$
12.0	$-0.30941E-03$	$-0.47603E-03$	$-0.78844E-03$
11.6	$-0.35772E-03$	$-0.55091E-03$	$-0.94534E-03$
11.4	$-0.38544E-03$	$-0.59391E-03$	$-0.10383E-02$
11.2	$-0.41594E-03$	$-0.64126E-03$	$-0.11418E-02$
11.0	$-0.44952E-03$	$-0.68441E-03$	$-0.12556E-02$
10.8	$-0.48661E-03$	$-0.73139E-03$	$-0.13774E-02$
10.6	$-0.52763E-03$	$-0.79883E-03$	$-0.15069E-02$
10.4	$-0.57310E-03$	$-0.87892E-03$	$-0.16414E-02$
10.2	$-0.62362E-03$	$-0.94478E-03$	$-0.17804E-02$
10.0	$-0.67990E-03$	$-0.10187E-02$	$-0.19236E-02$
9.8	$-0.74270E-03$	$-0.11247E-02$	$-0.20710E-02$
9.6	$-0.81924E-03$	$-0.12420E-02$	$-0.22248E-02$
9.4	$-0.90356E-03$	$-0.13738E-02$	$-0.23875E-02$
9.2	$-0.99641E-03$	$-0.15196E-02$	$-0.25644E-02$
9.0	$-0.10996E-02$	$-0.16738E-02$	$-0.27569E-02$
8.8	$-0.12174E-02$	$-0.18362E-02$	$-0.29699E-02$
8.6	$-0.13527E-02$	$-0.20115E-02$	$-0.32053E-02$
8.4	$-0.15075E-02$	$-0.22041E-02$	$-0.34653E-02$
8.2	$-0.16779E-02$	$-0.24144E-02$	$-0.37420E-02$
8.0	$-0.18604E-02$	$-0.26451E-02$	$-0.40182E-02$
7.8	$-0.20548E-02$	$-0.28970E-02$	$-0.42666E-02$
7.6	$-0.22612E-02$	$-0.31665E-02$	$-0.44567E-02$
7.4	$-0.24788E-02$	$-0.34457E-02$	$-0.45335E-02$
7.2	$-0.27014E-02$	$-0.37201E-02$	$-0.44437E-02$
7.0	$-0.29206E-02$	$-0.39729E-02$	$-0.40837E-02$
6.8	$-0.31132E-02$	$-0.41622E-02$	$-0.32855E-02$
6.6	$-0.32287E-02$	$-0.41980E-02$	$-0.19208E-02$
6.4	$-0.32022E-02$	$-0.39411E-02$	$0.57531E-04$
6.2	$-0.29173E-02$	$-0.32191E-02$	$0.29389E-02$
6.0	$-0.21994E-02$	$-0.18838E-02$	$0.66846E-02$
5.8	$-0.89017E-03$	$0.21120E-03$	$0.11814E-01$
5.6	$0.10842E-02$	$0.35725E-02$	$0.18266E-01$
5.4	$0.42119E-02$	$0.85351E-02$	$0.27361E-01$
5.2	$0.89691E-02$	$0.14888E-01$	$0.36828E-01$
5.0	$0.15353E-01$	$0.22943E-01$	$0.47733E-01$
4.8	$0.23267E-01$	$0.33776E-01$	$0.62593E-01$
4.6	$0.32120E-01$	$0.48083E-01$	$0.94514E-01$
4.3	$0.59612E-01$	$0.78169E-01$	$0.15969E+00$
4.0	$0.10774E+00$	$0.18298E+00$	$0.27010E+00$
3.5	$0.26973E+00$	$0.44684E+00$	$0.62604E+00$
3.0	$0.65194E+00$	$0.11082E+01$	$0.14478E+01$
2.5	$0.16125E+01$	$0.29034E+01$	$0.38801E+01$

variety of end effects in the mobility determination. Usually, four different drift distances are employed, and the variation in the drift velocities measured for different pairs of ion source positions is typically about 0.5%. Additional errors arise from temperature variation in the drift tube and from uncertainties in the pressure measurement. The pressures employed in the present research ranged between 0.020 and 0.400 torr. We estimate that the total absolute error in our final mobility determinations does not exceed ± 2%. Diffusion coefficients characterizing the dispersion of the ion bursts along the drift tube axis are obtained by matching the arrival time spectra to theoretical spectra calculated from the drift and diffusion parameters.[8] The match between the modeled and experimental spectra provides a sensitive test for experimental errors of several types, or for the presence of ion–molecule reactions. In the studies reported here, there is no evidence of reactions occurring. The reduced mobilities, as a function of E/N, are presented as points in Figs.
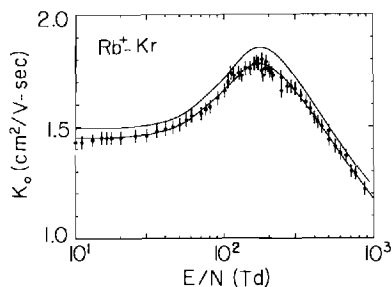
FIG. 2. The reduced mobility of Rb⁺ ions in kryton gas at 300 °K as a function of E/N in townsends (1 Td $= 10^{-17}$ V cm²). The experimental data are shown as points. The upper curve is the result of calculations using the Gordon–Waldman theoretical potential. The lower curve is the result of calculations using the directly determined potential given in Table I. Extrapolation to zero electric field yields a reduced mobility of 1.44, compared to the polarization limit mobility of 1.356 (all mobilities in cm²/V sec).
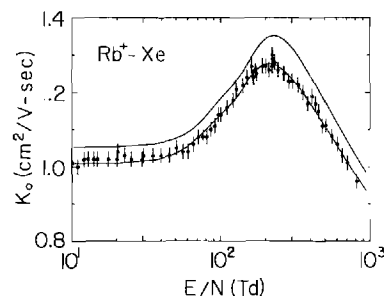

FIG. 3. The reduced mobility of Rb⁺ ions in xenon gas at 300 °K as a function of E/N in townsends (1 Td $= 10^{-17}$ V cm²). The experimental data are shown as points. The upper curve is the result of calculations using the Gordon–Waldman theoretical potential. The lower curve is the result of calculations using the directly determined potential given in Table I. Extrapolation to zero electric field yields a reduced mobility of 1.02, compared to the polarization limit mobility of 0.961 (all mobilities in cm²/V sec).

1, 2, and 3 for Rb⁺-Ar, Rb⁺-Kr, and Rb⁺-Xe respectively.

THEORY

Once the ion-neutral interaction potential has been specified, the ion mobilities as a function of E/N may be calculated theoretically using the nonequilibrium kinetic theory developed by Viehland and Mason.[1,2] This has been applied earlier to several alkali ion-rare gas combinations[9] including Rb⁺-Ar, using the potentials developed by Gordon and Waldman on an electron gas-Drude model basis.[10] The mobilities derived from these potentials for Rb⁺-Ar, Rb⁺-Kr, and Rb⁺-Xe are shown as the upper curves in Figs. 1, 2, and 3, respectively. A review of the procedures by which these are obtained is given in a similar paper on Cs⁺ ions in Ar, Kr, and Xe.[4]

DIRECTLY DETERMINED POTENTIALS

An inversion technique which combined the theoretical and experimental mobilities to refine the potential has

also been developed and applied to Li⁺-He and to Cs⁺-Ar, Cs⁺-Kr, and Cs⁺-Xe.[3,4,11] This leads to interaction potentials which are directly determined by the experimental mobilities for a range of internuclear separation distances from about 4 to about 10 a.u. (1 a.u. $= a_0$ $= 0.529$ Å). This range, of course, includes most of the potential well features. The long range potential is required to agree with the known polarization limit but the short range potential, being insensitive to the data, is treated as arbitrary in this analysis. The directly determined potentials for Rb⁺-Ar, Rb⁺-Kr, and Rb⁺-Xe are listed in Table I (the values for $r < 4$ a.u. indicate only what was used). The resulting mobilities are shown as the lower curves in Figs. 1–3.

DISCUSSION

A comparison of the Gordon–Waldman and the directly determined potentials is given in Table II, where the values of σ (the internuclear separation where the potential vanishes), r_m (the internuclear separation where the potential has its minimum), and V_m (the potential at r_m) are given. For Rb⁺-Ar and Rb⁺-Kr, both σ and r_m are increased by 5% in going from the theoretical to the experimental potential while V_m is reduced by 10%. For Rb⁺-Xe, the values of σ and r_m are increased by 10% and V_m is reduced by 25%. Within the context of the electron gas-Drude model calculations, the experiments indicate that the electron gas atom or ion is initially larger, or is less readily changed by the presence of the other particle than in the Gordon–Waldman theory.

TABLE II. The values of σ, r_m, and V_m for Rb⁺-Ar, Rb⁺-Kr, and Rb⁺-Xe interaction potentials as determined by the theory of Gordon and Waldman (G–W) and directly from experiment (D.D.). Atomic units are used (0.529 Å and 27.21 eV).

Gas	Potential	σ	r_m	V_m
Ar	G–W	5.4	6.3	−0.00360
Ar	D.D.	5.7	6.5	−0.00323
Kr	G–W	5.5	6.4	−0.00468
Kr	D.D.	5.8	6.7	−0.00420
Xe	G–W	5.7	6.7	−0.00602
Xe	D.D.	6.4	7.4	−0.00454

[1]L. A. Viehland and E. A. Mason, Ann. Phys (NY) **91**, 499 (1975).

[2]L. A. Viehland and E. A. Mason, Ann. Phys. (NY) **110**, 287 (1978).

[3]I. R. Gatland, W. F. Morrison, H. W. Ellis, M. G. Thackston, E. W. McDaniel, M. H. Alexander, L. A. Viehland, and E. A. Mason, J. Chem. Phys. **66**, 5121 (1977).

[4]I. R. Gatland, M. G. Thackston, W. M. Pope, F. L. Eisele, H. W. Ellis, and E. W. McDaniel, J. Chem. Phys. **68**, 2775 (1978).

[5]M. G. Thackston, H. W. Ellis, R. Y. Pai, and E. W. McDaniel, J. Chem. Phys. **65**, 2037 (1976).

[6]E. W. McDaniel and E. A. Mason, *The Mobility and Diffusion of Ions in Gases* (Wiley, New York, 1973).

[7]G. M. Thomson, J. H. Schummers, D. R. James, E. Graham, I. R. Gatland, M. R. Flannery, and E. W. McDaniel, J. Chem. Phys. **58**, 2402 (1973).

[8]I. R. Gatland, Case Stud. At. Phys. **4**, 369 (1974).

[9]I. R. Gatland, L. A. Viehland, and E. A. Mason, J. Chem. Phys. **66**, 537 (1977).

[10]M. Waldman and R. G. Gordon (private communication).

[11]L. A. Viehland, M. M. Harrington, and E. A. Mason, Chem. Phys. **17**, 433 (1976).

Mobilities and interaction potentials for Cs+–Ar, Cs+–Kr, and Cs+–Xe[a]

I. R. Gatland, M. G. Thackston, W. M. Pope, F. L. Eisele, H. W. Ellis, and E. W. McDaniel

School of Physics, Georgia Institute of Technology, Atlanta, Georgia 30332
(Received 25 November 1977)

The mobilities of Cs+ ions in Ar, Kr, and Xe gases at 300°K have been measured in a drift tube mass spectrometer for a wide range of values of the energy parameter E/N (the ratio of the electric field strength to the gas number density). Ion neutral interaction potentials have also been derived for each case (Cs+–Ar, Cs+–Kr, and Cs+–Xe). A kinetic theory appropriate to the nonthermalized ion motion is used to derive the mobilities from the potentials, and an iterative technique is used to modify the potentials to fit the experimental data. Various tests of the accuracy and uniqueness of the method indicate that this determination of the potentials gives errors in the potential parameters, e.g., well depth, well position, etc., which are less than about 10%.

INTRODUCTION

The transport properties of ions in neutral gases and in the presence of electric fields of arbitrary strength are intimately related to the ion–neutral interaction potential.[1,2] For ion–neutral potentials which are centrally symmetric, a knowledge of the potential is sufficient to accurately determine the ionic mobility[3] (v_d/E, where v_d is the ionic drift velocity and E is the electric field strength). Although the theory at present is not adequate to allow an immediate calculation of the potential from mobility data, an iterative inversion technique has been developed to obtain a potential which fits (i.e., accurately reproduces) the mobility data. The Li+–He system has recently been so treated,[4] and the resulting potential found to compare favorably with various *ab initio* theoretical potentials available for that system. In this paper we report measurements of the mobilities of Cs+ ions in Ar, Kr, and Xe gases, and use these data to derive an interaction potential in each case: Cs+–Ar, Cs+–Kr, and Cs+–Xe; systems for which *ab initio* theoretical potentials have not been reported.

EXPERIMENT

The mobilities of mass identified Cs+ ions in argon, krypton, and xenon have been measured using a drift tube mass spectrometer for a large range of values of E/N (the ratio of the electric field strength, E, to the neutral gas number density, N). The apparatus, which has been described previously,[5,6] measures the flight time for ions which are released from a source, drift and diffuse a known distance through a neutral gas at constant temperature and pressure in a uniform applied electric field, and then pass through a small aperture into a high vacuum region, where they are mass analyzed and detected. The differences between average drift times for various drift distances determine the drift velocity, v_d, and hence the mobility $K = v_d/E$. Since the mobility is inversely related to the number density of the neutral gas, the results are normalized to the density

at 760 torr and 0 °C. The result is the "reduced" mobility, K_0, where $K_0 = K(P/760)(273.16/T)$, and P and T are the pressure and temperature of the neutral gas in torr and degrees Kelvin, respectively. The technique of using several source positions (thereby changing the drift distance) and taking differences in flight times eliminates a variety of end effects from the final data.[7] At least three, and usually four, drift distances are used and the variation in the drift velocities measured for the different pairs is typically about 0.5%. Other errors arise from temperature variations in the drift tube and from uncertainties in the pressure measurement and result in an overall accuracy estimate of ±2%. Diffusion coefficients are obtained by matching the arrival time spectra to theoretical spectra calculated using the drift, diffusion, and reaction parameters. The match between the modeled and experimental spectra provides a sensitive test for experimental error, or the presence of unexpected reactions. In the present cases there are no discernible reactions. The diffusion results will be published separately. The reduced mobilities, as a function of E/N (the parameter that determines the average ion energy), are presented as experimental points
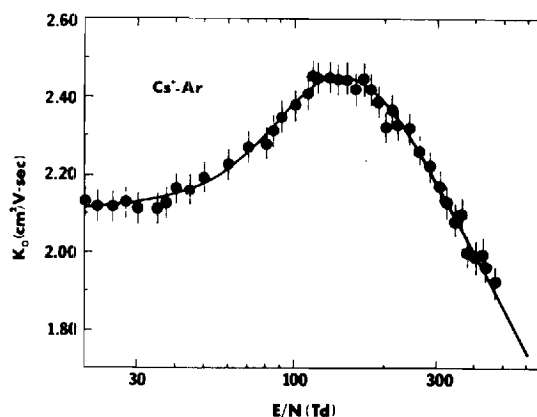

FIG. 1. The reduced mobility, K_0, of Cs+ ions in Ar as a function of E/N. The points represent the experimental measurements, while the curve is calculated using the interaction potential in Table I. The unit of E/N is the townsend, where 1 Td = 10^{-17} V-cm².
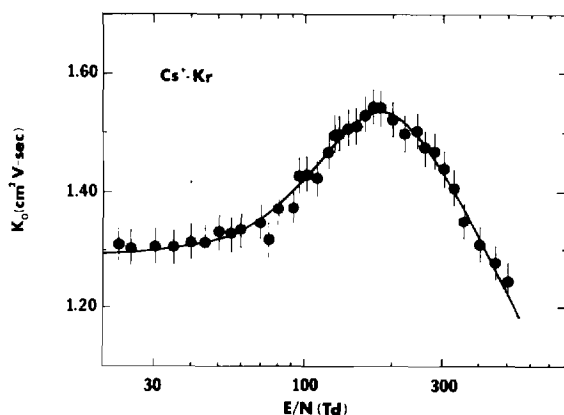
FIG. 2. The reduced mobility, K_0, of Cs⁺ ions in Kr as a function of E/N. The points represent the experimental measurements, while the curve is calculated using the interaction potential in Table I. The unit of E/N is the townsend, where $1\ Td = 10^{-17}\ V\text{-}cm^2$.

in Figs. 1, 2, and 3 for Cs⁺ in Ar, Kr, and Xe, respectively. In all cases the gas temperature was 300 °K.

THEORY

The fundamental use of ion mobility measurements requires a theory which determines the mobility for any specified ion–neutral interaction potential. Such a theory has been developed by Viehland and Mason for centrally symmetric potentials with mobilities at arbitrary electric field strengths.[1,2] The salient features of the theory are as follows.

Given a theoretical or test potential, the transport cross sections are calculated by classical or quantum mechanical methods using the definitions

$$Q_l(\epsilon) = \left(1 + \frac{1 + (-1)^l}{2l}\right) \int [1 - \cos^l\theta(\epsilon, b)] 2\pi b\, db$$

$$= \left(1 + \frac{1 + (-1)^l}{2l}\right) \int (1 - \cos^l\theta)\sigma(\epsilon, \theta)\, d\Omega$$

for a range of energies ϵ where σ is the differential cross section for scattering through an angle θ. Then the omega integrals are evaluated for a range of temperatures, T,

$$\Omega^{(l, s)}(T) = ((s + 1)!)^{-1} \int_0^\infty Q_l(kTx)e^{-x}x^{s+1}\, dx ,$$

where k is Boltzmann's constant. These omega integrals are used in the kinetic theory describing the ionic motion.

The Boltzmann equation, which determines the ion velocity distribution is solved by the moment method using as a basis the Burnett functions

$$\psi_l^r(\mathbf{v}) = L_r^{l+1/2}(w^2)w^l P_l(w_z/w) ,$$

where L and P are the associated Laguerre and Legendre polynomials, respectively. The vector $\mathbf{w}$ is related to $\mathbf{v}$ by

$$\mathbf{w} = (m/2kT_i)^{1/2}\mathbf{v} ,$$

and the moment equations are made to converge rapidly by choosing T_i to be a temperature appropriate to the ions. For this purpose the implicit subsidiary condition

$$\tfrac{3}{2}kT_i = \tfrac{1}{2}m\langle v^2 \rangle$$

is chosen, where m is the ion mass and $\langle\ \rangle$ represents an average over the velocity distribution. Then the moment equations are

$$\frac{eE}{mN}\left\langle\frac{d\psi_l^r}{dv_z}\right\rangle = \langle J\psi_l^r \rangle ,$$

where J is the collision operator defined by[8]

$$J\psi = N^{-1} \int F(V)[\psi(\mathbf{v}) - \psi(\mathbf{v}')]|\mathbf{v} - \mathbf{V}|\sigma\, d\Omega d^3V ,$$

with F the neutral gas velocity distribution (assumed to be Maxwell–Boltzmann). Since the Burnett functions are complete, both $d\psi_l^r/dv_z$ and $J\psi_l^r$ can be expanded in terms of the ψ's. In particular,

$$J\psi_l^r = \sum_s a_{rs}(l)\psi_l^s ,$$

with

$$a_{rs}(l) = \frac{(2l + 1)\Gamma(\tfrac{3}{2})s!}{\Gamma(l + s + \tfrac{3}{2})\pi^{3/2}} \int e^{-w^2}\psi_l^s J\psi_l^r\, d^3w .$$

The matrix elements of the collision operator, $a_{rs}(l)$, may be evaluated in terms of the omega integrals at a temperature which describes the ion–neutral collisions, T_f, defined by

$$T_f = (T/M + T_i/m)\mu ,$$

where M is the neutral mass and $\mu = mM/(m + M)$ is the reduced mass. In particular,

$$a_{00}(1) = \tfrac{8}{3}m^{-1}(2kT_f\mu/\pi)^{1/2}\Omega^{(1, 1)}(T_f) ,$$

and

$$a_{10}(0) = -8(MT_i)^{-1}(T_f - T)(2kT_f\mu/\pi)^{1/2}\Omega^{(1, 1)}(T_f) .$$
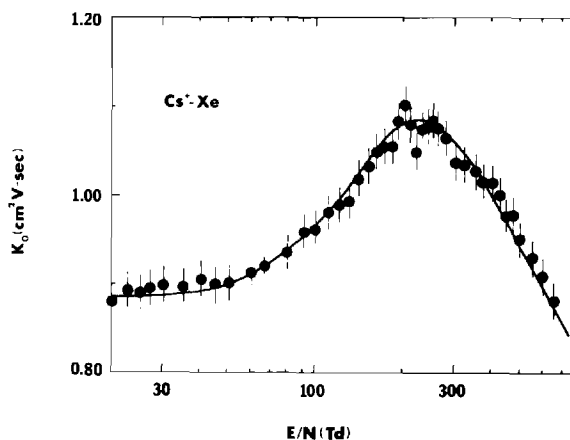
In expanded form the moment equations become

FIG. 3. The reduced mobility, K_0, of Cs⁺ ions in Xe as a function of E/N. The points represent the experimental measurements, while the curve is calculated using the interaction potential in Table I. The unit of E/N is the townsend, where $1\ Td = 10^{-17}\ V\text{-}cm^2$.

$$\gamma\left(\frac{l(\gamma+l+\frac{1}{2})}{(l+\frac{1}{2})}\langle\psi_{l-1}^r\rangle - \frac{l+1}{l+\frac{1}{2}}\langle\psi_{l+1}^r\rangle\right) = \sum_s \frac{a_{rs}(l)}{a_{00}(1)}\langle\psi_l^s\rangle,$$

with

$$\gamma = (m/2kT_i)^{1/2} eE/N m a_{00}(1),$$

where e is the ionic charge. The subsidiary condition defining T_i requires that γ (i.e. E/N) be treated as an unknown quantity so that the infinite set of moment equations is also nonlinear. To effect a solution a particular value of T_f (and hence T_i) is assumed and the moment equations are truncated and solved by iteration to give values for γ and $\langle\psi_1^0\rangle$ from which E/N and $v_d = \langle v\rangle$ are obtained. The first order result

$$\gamma = \langle\psi_1^0\rangle = [-a_{10}(0)/2a_{00}(1)]^{1/2}$$

yields

$$v_d = \frac{3eE}{8N(2kT_f\mu/\pi)^{1/2}\Omega^{(1,1)}(T_f)}$$

and

$$\tfrac{3}{2}kT_f = \tfrac{3}{2}kT + \tfrac{1}{2}Mv_d^2,$$

where T, the neutral gas temperature, is 300 °K for all cases discussed here. Unfortunately the error in the first order calculation is typically 10% and in general third order results are required to reduce the error below 1%. All results presented here are based on third order calculations, i.e., matrix elements with r or s greater than 3 are taken to be zero. Thus, using a range of effective temperatures, T_f, a table of E/N and K_0 can be generated and compared with experimental results.

INVERSION PROCEDURE

For interactions for which a theoretical ground state potential is known the mobility measurements provide a sensitive test of the potential for collision energies in the range 0.03–1.0 eV. We also need, however, a method of developing the potential directly from the mobility data. An inversion technique has been proposed by Mason and Viehland[9] based on the methods of E. B. Smith.[10] Using a trial potential one obtains a trial mobility curve. Then, using the first order formulas, values of T_f are selected and E/N, K_0 and hence $\Omega^{(1,1)}$ are found. Then an effective radius $r_t = (\Omega^{(1,1)}/\pi)^{1/2}$ and the ratio $\xi = V(r_t)/T_f$ are calculated. Next one repeats the calculation using the experimental mobilities to obtain an effective radius r_e. Finally, a new potential value is determined using $V(r_e) = \xi T_f$, and a new mobility curve generated. This procedure may be iterated to improve the fit to the experimental data. The procedure effectively warps the radial distance scale but cannot change the potential well depth. A change in the energy scale must be included separately by using, say, $V(r) \to \eta V(r)$. Two methods have been proposed to determine the best potential well depth. That of Maitland *et al.*[11] adopts the well depth which gives the fastest convergence of the theoretical to the experimental mobilities as the inversion procedure is iterated. The method we have developed depends on the observation that the mobility peak changes position (as a function of T_f) as the well depth is varied. This latter technique has the advantage of indicating the sign,

and to some extent the magnitude, of the required change. We have used both methods in these studies; the latter to change the well depth and the former to check that the well depth is correct.

Since the mobility data only cover a finite range of energies (kT_f) the long and short range parts of the potential are not fixed by the data. The long range part is already well known from the polarization potential but the short range behavior has to be assumed, or higher energy experiments such as beam experiments have to be used. No such high energy data are available in the present cases so the short range part of the potentials that we obtain are dependent on the initial trial potentials.

RESULTS

For each case (Cs⁺-Ar, Cs⁺-Kr, and Cs⁺-Xe), potentials were obtained from the mobility data using a

TABLE I. Interaction potential for Cs⁺ ions with Ar, Kr, and Xe, obtained by directly inverting the mobility data. Both the distance and the potential are in atomic units (i.e., 0.52917 Å and 27.211 eV).

R	Cs⁺-Ar	Cs⁺-Kr	Cs⁺-Xe
15.0	−0.00012251	−0.00018166	−0.00031258
14.5	−0.00014135	−0.00020936	−0.00036143
14.0	−0.00016398	−0.00024259	−0.00042031
13.5	−0.00019136	−0.00028273	−0.00049179
13.0	−0.00022476	−0.00033161	−0.00057932
12.5	−0.00026586	−0.00039162	−0.00068742
12.0	−0.00031689	−0.00046597	−0.00084967
11.6	−0.00036690	−0.00053867	−0.0010016
11.2	−0.00042727	−0.00062625	−0.0011854
10.8	−0.00050070	−0.00073360	−0.0014117
10.4	−0.00059077	−0.00086656	−0.0016852
10.0	−0.00070226	−0.0010437	−0.0020059
9.8	−0.00076672	−0.0011517	−0.0021815
9.6	−0.00084060	−0.0012777	−0.0023670
9.4	−0.00092415	−0.0014147	−0.0025586
9.2	−0.0010180	−0.0015547	−0.0027576
9.0	−0.0011245	−0.0017005	−0.0029612
8.8	−0.0012498	−0.0018567	−0.0031660
8.6	−0.0013910	−0.0020231	−0.0033606
8.4	−0.0015483	−0.0022010	−0.0035521
8.2	−0.0017235	−0.0023993	−0.0037315
8.0	−0.0019179	−0.0026313	−0.0038844
7.8	−0.0021251	−0.0028919	−0.0039834
7.6	−0.0023394	−0.0031737	−0.0039864
7.4	−0.0025554	−0.0034735	−0.0038346
7.2	−0.0027575	−0.0037805	−0.0034294
7.0	−0.0029321	−0.0040756	−0.0026369
6.8	−0.0030590	−0.0043158	−0.0013579
6.6	−0.0030975	−0.0044460	0.0007065
6.4	−0.0029727	−0.0043483	0.0039969
6.2	−0.0025690	−0.0038076	0.0083533
6.0	−0.0017128	−0.0024717	0.013191
5.8	−0.0001758	0.0001610	0.019894
5.6	0.0024618	0.0044058	0.028749
5.4	0.0065520	0.012535	0.039901
5.2	0.013146	0.032581	0.057984
5.0	0.023778	0.054716	0.091165
4.8	0.040316	0.10483	0.14641
4.6	0.062865	0.19470	0.23618
4.4	0.099512	0.35802	0.38436
4.2	0.16222	0.66026	0.63345
4.0	0.26420	1.2323	1.06110

trial potential of the 4–6–n type

$$V = -C_4/r^4 - C_6/r^6 + C_n/r^n$$

with C_4 given by the polarization limit, $n = 12$ initially, and C_6 and C_n chosen to give reasonable values of the potential well depth and position. The inversion procedure changes the well position and gives a potential which is not of the 4–6–n type in general. The well depth and the value of n are varied to obtain a good fit with few iterations. Typically the uncertainty in the well depth is about 10% with the present data, and this uncertainty carries over into the estimate of the well position, etc. The potentials are given in Table I with both r and V in atomic units (0.529 Å and 27.21 eV). The values at the end of the table are included for definiteness but are not directly determined by the experimental data. The minimum distances affected by the data are $r = 4.5$ au for Cs^+-Ar, $r = 5.0$ au for Cs^+-Kr, and $r = 5.0$ au for Cs^+-Xe. The resulting mobilities are shown as curves in Figs. 1, 2, and 3 for comparison with the experimental data.

A number of checks have been applied to the kinetic theory calculations. Selected omega integrals have been calculated both by our program and by that of O'Hara and Smith[12] and found to agree to within 0.2%. Some mobilities have been obtained using the fourth order approximation in the kinetic theory, as well as third order, with less than 0.5% change. Attempts to obtain fits starting with trial potentials having well depths which are 20% different from the best case have consistently failed. However, obtaining a directly determined potential does depend on the range of the data. If the range is too narrow the energy integration associated with the omega integrals cannot be unfolded. Also, for a potential with a shallow well, the minimum experimental energy (thermal) may be too high so that the data only relate to the repulsive part of the potential. This appears to be the case for Cs^+-He and Cs^+-Ne. Experiments at temperatures below 100 °K should obviate this problem. For the argon, krypton, and xenon cases the mobilities at thermal temperatures are close to the polarization limit. The zero field reduced mobilities at 300 °K and the reduced polarization mobilities, respectively, are 2.11 and 1.95 for Cs^+-Ar, 1.30 and 1.23 for Cs^+-Kr, and 0.89 and 0.85 for Cs^+-Xe (all mobilities in cm^2/V sec).

ACKNOWLEDGMENTS

[1]L. A. Viehland and E. A. Mason, Ann. Phys. (NY) **91**, 499 (1975).

[2]L. A. Viehland and E. A. Mason, Ann. Phys. (NY) (to be published).

[3]I. R. Gatland, L. A. Viehland, and E. A. Mason, J. Chem. Phys. **66**, 537 (1977).

[4]I. R. Gatland, W. F. Morrison, H. W. Ellis, M. G. Thackston, E. W. McDaniel, M. H. Alexander, L. A. Viehland, and E. A. Mason, J. Chem. Phys. 66, 5121 (1977).

[5]G. M. Thomson, J. H. Schummers, D. R. James, E. Graham, I. R. Gatland, M. R. Flannery, and E. W. McDaniel, J. Chem. Phys. **58**, 2404 (1973).

[6]E. W. McDaniel and E. A. Mason, *The Mobility and Diffusion of Ions in Gases* (Wiley, New York, 1973).

[7]I. R. Gatland, Case Stud. At. Phys. 4, 369 (1974).

[8]S. Chapman and T. G. Cowling, *The Mathematical Theory of Non-Uniform Gases* (Cambridge University, London, 1952), 2nd ed.

[9]L. A. Viehland, M. M. Harrington, and E. A. Mason, Chem. Phys. **17**, 433 (1976).

[10]E. B. Smith, Physica (Utr.) **73**, 211 (1974).

[11]G. C. Maitland, E. A. Mason, L. A. Viehland, and W. A. Wakeham (private communication).

[12]H. O'Hara and F. J. Smith, J. Comput. Phys. **5**, 328 (1970).